



Development of a fiber-optic gamma endoscope to measure both optical and gamma images in a confined space

MINGEON KIM,¹ WOOK JAE YOO,² AND BONGSOO LEE^{1,*}

¹*School of Energy Systems Engineering, Chung-Ang University, Heukseok-dong, Dongjak-gu, Seoul 156-756, South Korea*

²*School of Biomedical Engineering, College of Biomedical & Health Science, BK21 Plus Research Institute of Biomedical Engineering, Konkuk University, Chungju 380-701, South Korea*

*bslee@cau.ac.kr

Abstract: In nuclear medicine, obtaining information on the exact location, size, and dose of radiopharmaceuticals distributed on lesions is critically important. Therefore, we have fabricated a novel fiber-optic gamma endoscope (FOGE) to measure the shape and size of the radioisotope as well as the gamma-ray distribution simultaneously. To evaluate the performance of the novel FOGE, we obtained optical images and gamma images by using a USAF 1951 target and radioisotope sources, respectively. The experimental results demonstrated that the FOGE could be utilized to obtain both the location and the distribution of the radioactive isotope that emitted gamma-rays. Based on the results of this study, use of a flexible and thin FOGE would be valuable in nuclear medicine and nuclear safety technologies given the advantages of accurate dose-monitoring. Especially, improvements could be achieved in surgery technologies because the FOGE could be used in minimally invasive radioguided surgery owing to its thin form and flexibility.

© 2017 Optical Society of America

OCIS codes: (060.2350) Fiber optics imaging; (060.2370) Fiber optics sensors; (220.0220) Optical design and fabrication; (170.2670) Gamma ray imaging; (120.4610) Optical fabrication.

References and links

1. V. Desiato, M. Melis, B. Amato, T. Bianco, A. Rocca, M. Amato, G. Quarto, and G. Benassai, "Minimally invasive radioguided parathyroid surgery: A literature review," *Int. J. Surg.* **28**, S84–S93 (2016).
2. A. J. Coakley, A. G. Kettle, C. P. Wells, M. J. O'Doherty, and R. E. Collins, "99m-Tc sestamibi: a new agent for parathyroid imaging," *Nucl. Med. Commun.* **10**(11), 791–794 (1989).
3. M. J. O'Doherty, A. G. Kettle, P. Wells, R. E. C. Collins, and A. J. Coakley, "Parathyroid imaging with technetium-99m-sestamibi: preoperative localization and tissue uptake studies," *J. Nucl. Med.* **33**(3), 313–318 (1992).
4. O. Geatti, B. Shapiro, P. G. Orsolon, G. Proto, U. P. Guerra, F. Antonucci, and D. Gasparini, "Localization of parathyroid enlargement: experience with 99mtechnetium methoxyisobutylisonitrile and thallium-201 scintigraphy, ultrasonography and computed tomography," *Eur. J. Nucl. Med.* **21**(1), 17–22 (1994).
5. F. L. Moffat, Jr., "Targeting gold at the end of the rainbow: surgical gamma probes in the 21st century," *J. Surg. Oncol.* **96**(4), 286–289 (2007).
6. N. C. Hall, S. P. Povoski, D. A. Murrey, Jr., M. V. Knopp, and E. W. Martin, Jr., "Bringing advanced medical imaging into the operative arena could revolutionize the surgical care of cancer patients," *Expert Rev. Med. Devices* **5**(6), 663–667 (2008).
7. D. Rubello, A. Piotto, D. Casara, P. C. Muzzio, B. Shapiro, and M. R. Pelizzo, "Role of gamma probes in performing minimally invasive parathyroidectomy in patients with primary hyperparathyroidism: optimization of preoperative and intraoperative procedures," *Eur. J. Endocrinol.* **149**(1), 7–15 (2003).
8. D. Casara, D. Rubello, M. R. Pelizzo, and B. Shapiro, "Clinical role of 99mTcO4/MIBI scan, ultrasound and intra-operative gamma probe in the performance of unilateral and minimally invasive surgery in primary hyperparathyroidism," *Eur. J. Nucl. Med.* **28**(9), 1351–1359 (2001).
9. D. Rubello, D. Casara, S. Giannini, A. Piotto, E. De Carlo, P. C. Muzzio, and M. R. Pelizzo, "Importance of radio-guided minimally invasive parathyroidectomy using hand-held gamma probe and low (99m)Tc-MIBI dose. Technical considerations and long-term clinical results," *Q. J. Nucl. Med.* **47**(2), 129–138 (2003).
10. J. Norman, H. Chheda, and C. Farrell, "Minimally invasive parathyroidectomy for primary hyperparathyroidism: decreasing operative time and potential complications while improving cosmetic results," *Am. Surg.* **64**(5), 391–395 (1998).

11. Blog, Minimally invasive heart surgery, “Advantages and Disadvantages of Minimally Invasive Surgery,” (Minimally Invasive and Bloodless Heart Surgery Center 2016), <http://heartsurgeryinfo.com/advantages-and-disadvantages-of-minimally-invasive-surgery/>
12. Product information, “Gamma Probes,” (IMI Intramedical Imaging), <http://www.gammaprobe.com/products/gamma-probes/>
13. Criteria for gamma probe systems, “Crystal Probe,” (Crystal Photonics), <http://crystal-photonics.com/enu/solutions/criteria-enu.htm>
14. I. Sarikaya, A. Sarikaya, and R. C. Reba, “Gamma probes and their use in tumor detection in colorectal cancer,” *Int. Semin. Surg. Oncol.* **5**(5), 25 (2008).
15. R. Garcia-Parra, N. Clinthorne, L. Wang, M. Picchio, and M. Piert, “Performance of beta- and high-energy gamma probes for the detection of cancer tissue in experimental surgical resection beds,” *Ann. Nucl. Med.* **25**(7), 486–493 (2011).
16. R. R. Raylman, S. J. Fisher, R. S. Brown, S. P. Ethier, and R. L. Wahl, “Fluorine-18-fluorodeoxyglucose-guided breast cancer surgery with a positron-sensitive probe: validation in preclinical studies,” *J. Nucl. Med.* **36**(10), 1869–1874 (1995).
17. K. T. Han, W. J. Yoo, J. K. Seo, S. H. Shin, D. Jeon, S. Hong, S. Cho, J. H. Moon, and B. Lee, “Optical fiber-based gamma-ray spectroscopy with cerium-doped lutetium yttrium orthosilicate crystal,” *Opt. Rev.* **20**(2), 205–208 (2013).
18. K. W. Jang, T. Yagi, C. H. Pyeon, W. J. Yoo, S. H. Shin, T. Misawa, and B. Lee, “Feasibility of fiber-optic radiation sensor using Cerenkov effect for detecting thermal neutrons,” *Opt. Express* **21**(12), 14573–14582 (2013).
19. A. F. Fernandez, B. Brichard, S. O’Keeffe, C. Fitzpatrick, E. Lewis, J.-R. Vaille, L. Dusseau, D. A. Jackson, F. Ravotti, M. Glaser, and H. El-Rabii, “Real-time fiber optic radiation dosimeters for nuclear environment monitoring around thermonuclear reactors,” *Fusion Eng. Des.* **83**(1), 50–59 (2008).
20. S. O’Keeffe, C. Fitzpatrick, E. Lewis, and A. I. Al-Shamma’a, “A review of optical fibre radiation dosimeters,” *Sens. Rev.* **28**(2), 136–142 (2008).
21. B. Lee, K. W. Jang, D. H. Cho, W. J. Yoo, S. H. Shin, G.-R. Tack, S.-C. Chung, S. Kim, H. Cho, B. G. Park, J. H. Moon, and S. Kim, “Characterization of one-dimensional fiber-optic scintillating detectors for electron-beam therapy dosimetry,” *IEEE Trans. Nucl. Sci.* **55**(5), 2627–2631 (2008).
22. K. W. Jang, D. H. Cho, W. J. Yoo, J. K. Seo, J. Y. Heo, J.-Y. Park, and B. Lee, “Fiber-optic radiation sensor for detection of tritium,” *Nucl. Instrum. Methods Phys. Res. A* **652**(1), 928–931 (2011).
23. H. Bueker and F. W. Haesing, “Fiber optic radiation sensors,” *Opt. Fibre Sens. and Syst. in Nucl. Environments* **2425**(106), 106 (1994).
24. D. H. Cho, K. W. Jang, W. J. Yoo, S. C. Chung, G. R. Tack, G. M. Eom, B. Lee, H. Cho, and S. Kim, “Performance Evaluation of One-dimensional Fiber-optic Radiation Sensor for Measuring High Energy Electron Beam Using a Charge-coupled Device,” *J. Nucl. Sci. Technol.* **45**(sup5), 477–480 (2008).
25. Y. M. Hwang, D. H. Cho, B. Lee, H. S. Cho, and S. Kim, “Fabrication and characterization of plastic fiber-optic radiation sensor tips using inorganic scintillator material,” *J. Sens. Sci. Technol.* **14**(4), 244–249 (2005).
26. H.-G. Kang, K. M. Kim, H.-Y. Lee, G. C. Hong, H. S. Lee, and S. J. Hong, “A feasibility study of simultaneous endoscopic NIR/gamma/visible fusion imaging for intraoperative surgery,” *J. Nucl. Med.* **56**, 606 (2015).
27. H.-G. Kang, H.-Y. Lee, K. M. Kim, S.-H. Song, G. C. Hong, and S. J. Hong, “A feasibility study of an integrated NIR/gamma/visible imaging system for endoscopic sentinel lymph node mapping,” *Med. Phys.* **44**(1), 227–239 (2017).
28. Product information, “BGO, LYSO and GSO crystal scintillators,” (Omega Piezo), http://www.omegapiezo.com/crystal_scintillators.html
29. K. W. Jang, D. H. Cho, W. J. Yoo, B. Lee, J.-H. Moon, B.-G. Park, Y.-H. Cho, and S. Kim, “Fabrication and characterization of a fiber-optic radiation sensor for detection of tritium,” *Korean J. Opt. Photon.* **20**(4), 201–206 (2009).

1. Introduction

Recently, the minimally invasive approach has become widely used in the field of radioguided surgery [1]. Minimally invasive radioguided surgery (MIRS) has been performed by using imaging techniques such as methoxyisobutylisonitrile (MIBI, also called sestamibi) scintigraphy, ultrasonography, computed tomography (CT)-scanning, magnetic resonance imaging (MRI), and single-photon emission computed tomography (SPECT), which all have contributed to the development of exploration approaches and enabled the accurate identification of abnormal lesions preoperatively [2–4]. Along with these preoperative imaging techniques, increasingly advanced gamma probes have been made available, thus providing for the possibility of easy intraoperative identification of lesions [5, 6]. It is clear that gamma-probe scanning is indispensable when surgical access areas are small [7]. During MIRS, the gamma probe is used to measure radioactivity of radiopharmaceuticals distributed over the whole lesion accurately, and once the lesion spot is confirmed, a small incision

(usually around 2–2.5 cm) is performed [8, 9]. It has been reported that MIRS can reduce costs and operative times, enable medical providers to carry out procedures with fewer complications and smaller incisions, and produce comparable operative success rates [10]. However, MIRS requires more expensive high-end medical equipment and surgeons with specialized training. Moreover, some operations may actually take longer because of the various procedures involved [11]. Therefore, to make MIRS surgery safer and more commercializable, it is necessary to develop an intraoperative gamma probe that is smaller and easier to handle for the most experienced surgeon. Gamma probes used in hospitals currently have several disadvantages when they are applied to MIRS. The commercialized gamma probes are usually as large as 12 mm, and the smallest diameter of a commercial gamma probe is 5 mm. To perform more effective MIRS, the development of smaller gamma probes would be desirable [12]. Further, gamma probes currently in clinical use are vulnerable to electromagnetic fields because scintillators sensing gamma-rays are directly connected to photodiodes that convert data into electrical signals, and thus, they have a disadvantage in that only a single type of radiation can be detected. In addition, gamma probes typically have a spatial resolution that is not enough to accurately detect small lesions distributed in the parathyroid lymph node and glands in MIRS [13]. Also, there is a further disadvantage in that the setup requires electronic equipment with position-encoding circuits [14–16].

Recently, a fiber-optic based radiation detector has been developed to overcome the disadvantages of conventional gamma probes. Fiber-optic based detectors have the advantages of miniaturization, high spatial resolution, long length of transmission, and no interference of electromagnetic fields [17–21]. However, in spite of the various advantages of fiber-optic-based radiation detectors, fiber-optic gamma probes developed thus far can only be used to determine the presence and radioactivity of radionuclides by using the intensity of light signals emitted from the scintillator [22–25]. Also, there were previous works to demonstrate the feasibility of simultaneous endoscopic optical and gamma imaging system. However their fusion imaging probe cannot be used in MIRS due to pretty big size of distal end including a tungsten pinhole collimator [26, 27].

The purpose of this study is to fabricate a novel fiber-optic gamma endoscope (FOGE) for obtaining both optical and gamma images that can be used in MIRS. The proposed FOGE is based on a high-transparency and high-light-yielding scintillator that transmits the optical images and produces scintillating lights referred to here as gamma images. Moreover, this FOGE can be miniaturized and can detect the location of a radioisotope. We can obtain both optical and gamma images with a very simple method in confined spaces such as small incisions during MIRS when using this instrument. This novel FOGE is expected to provide important information during the identification of lesions with small incisions and will be easy to handle for experienced surgeons because it can be used in an examination with optical images. The ability to obtain both optical and gamma images simultaneously with high resolution and sensitivity during surgery also will enable the surgeons to visualize and find lesions very easily and quickly.

2. Methods and materials

The novel FOGE system is comprised of UV filter film (#39-426, Edmunds Optics), an imaging lens (ILW-2.00, GoFoton), a scintillator disc (Epic Crystal), a coherent image guide (MCL-2000-2.4, Industrial Optics), a fiber-optic taper (#55-141, Edmunds Optics), an image intensifier (BV 2538 BZ-V, Proxivision), and a complementary metal-oxide semiconductor (CMOS) camera module (UI-1480SE-C-HQ, iDS).

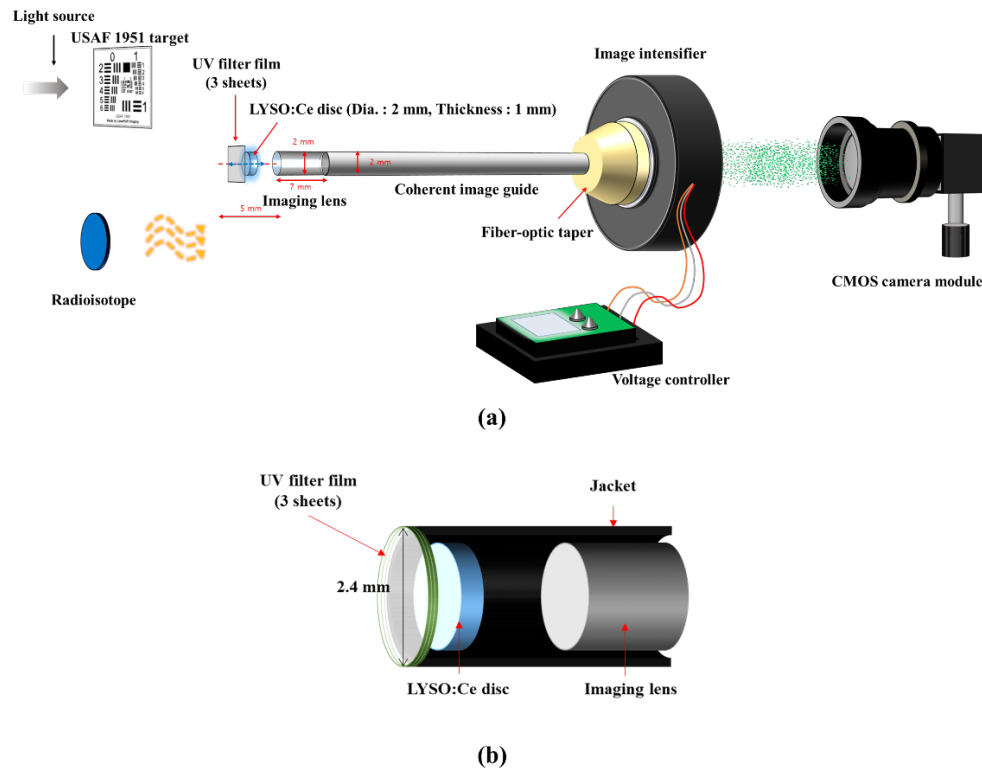


Fig. 1. (a) Experimental setup of the FOGE and (b) inner structure of the distal-end of the FOGE.

Figure 1(a) shows the experimental setup of the fabricated FOGE, whose outer diameter and length are 2.0 and 300 mm, respectively. To obtain gamma and optical images, a transparent and thin scintillator disc and an optical imaging lens with arraying in a line are employed as the main elements at the distal end of the FOGE. The imaging lens is commonly used as an objective lens for small-diameter imaging systems, where conventional lenses are not suitable, owing to size limitations. The diameter and pitch of the lens used in this study are 2.0 mm and 0.23, respectively.

As a scintillator disc, cerium-doped lutetium yttrium orthosilicate (LYSO:Ce) crystal with a thickness of 1 mm and diameter of 2 mm is used to transmit the optical image and to produce the scintillating lights, owing to its high transparency and light yield [28]. In addition, this small LYSO:Ce disc should be moved forward or backward to focus the gamma image and the optical image. As shown in Fig. 1(b), the tip of the FOGE is covered by three sheets of UV filter film to prevent the excitation of LYSO:Ce by UV light and these films are attached to the LYSO:Ce disc using an optical epoxy and index matching oil. Finally, the optical image can be acquired by using an imaging lens, and it is transmitted to a fiber-optic taper and a CCD camera module through a fiber-optic image guide. In general, a coherent image guide is an assembly of micro-optical fibers, in which the individual optical fibers are stacked in the same direction at both ends of the image guide. The coherent image guide used in this endoscope has an outer diameter of 2.0 mm and consists of 13,000 polymethyl methacrylate (PMMA) and fluorinated-polymer (FP)-based micro optical fibers with a diameter of 8.7 μm , and the refractive indices of the core and cladding of an individual optical fiber are 1.49 and 1.40, respectively. The numerical aperture (NA) of an individual optical fiber is about 0.5, and the spatial resolution of the coherent image guide is about 57.4 lp/mm.

A fiber-optic taper was also used as an image guide in this study to transmit a 2.27 times magnified image from the outer surface of the coherent image guide to its output surface. The diameter of the large end and the size of the small end of the taper were 27 mm and 6.4×4.8 mm², respectively. The NA was approximately 1.00, and its spatial resolution was 102 lp/mm. To reduce distortion and achieve high-contrast image quality for the fiber-optic taper, the individual fiber was made with an extra-mural absorption (EMA) material that minimized leaky rays. In addition, we also coated optical index matching oil on all optical interfaces of the FOGE to reduce leaky rays.

As shown in Fig. 1(a), the gamma image is generated in the scintillating disc, and it is also transmitted through the imaging lens, coherent image guide, and fiber-optic taper to the image intensifier. The light intensity of the magnified scintillation image is intensified by the image intensifier with a high spectral gain of 3.3×10^6 and high quantum efficiency. The phosphor screen of the image intensifier is composed of terbium-doped gadolinium oxysulfide (Gd₂O₂S:Tb), in which an amplified image with a light emission peak of 545 nm is transmitted to the output window of the image intensifier. Furthermore, the image intensifier has a spatial resolution of 28 lp/mm owing to the fiber-optic plates at the input and output windows, which can transmit a gamma image without any image distortion. The intensified scintillation image is captured by the CMOS image sensor with a fixed focal length lens and a 2X extender over a certain period. Subsequently, video files containing the information on the gamma images are converted to a red-green-blue (RGB) color image map by using the MATLAB program (MATLAB, MathWorks).

3. Experimental setup and results

In this study, to evaluate the performance of the novel FOGE, we obtained optical images and gamma images by using an USAF 1951 target and radioisotope sources, respectively. From the optical images, we measured the spatial resolutions of this optical system in relation to the groups and elements of a USAF 1951 target and through modulation transfer function (MTF) calculations. From the gamma images, we also measured the gamma distribution images of radioisotopes with different radioactivity.

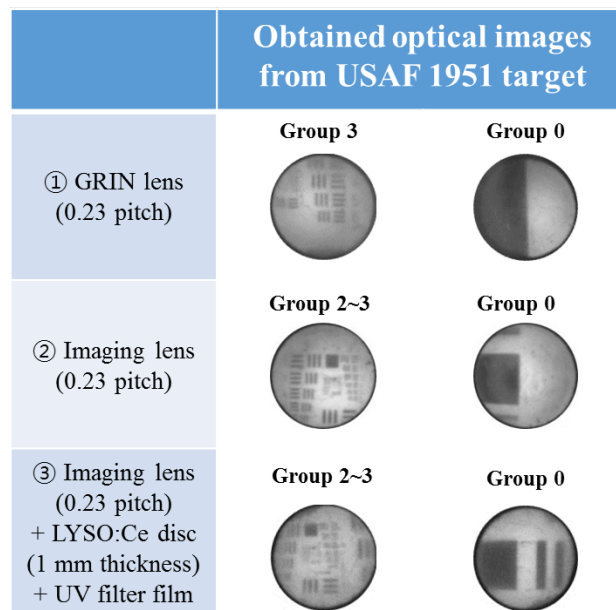


Fig. 2. Optical images from the USAF 1951 target according to the optical system.

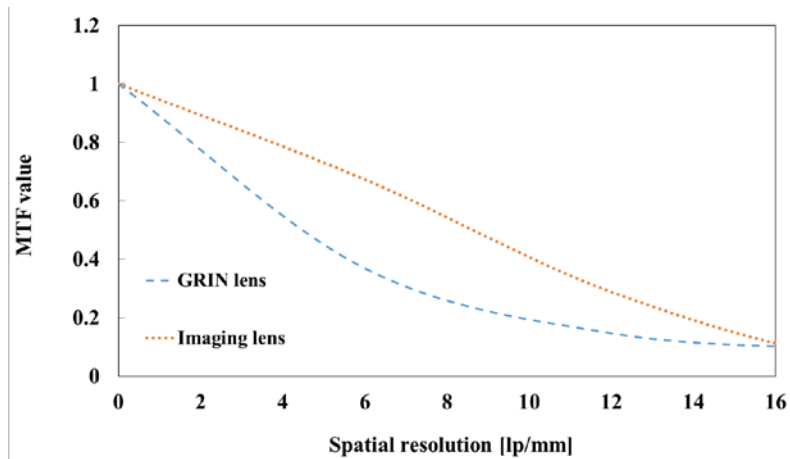


Fig. 3. MTF curves when only one types of GRIN lens or imaging lens is used.

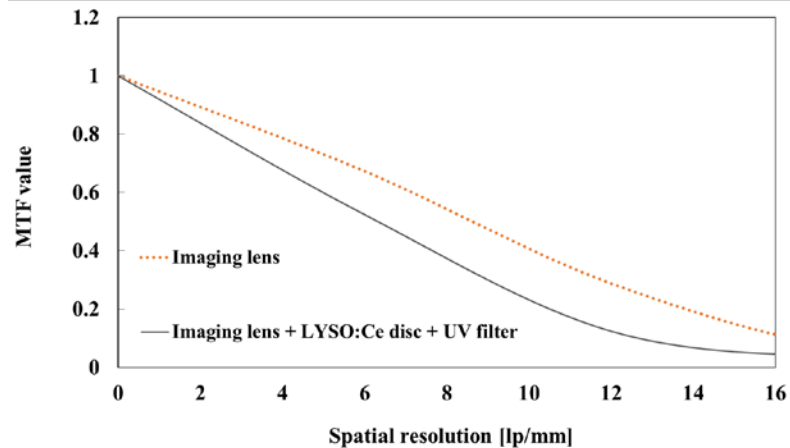


Fig. 4. MTF curves according to the optical system.

Figure 2 shows the groups and elements of a USAF 1951 target according to the component of the optical system applied in the FOG. As shown in Fig. 2-1, we can clearly see the magnified group 3 of the USAF 1951 target when the graded-index (GRIN) lens with a 0.23 pitch is arrayed in the FOG. On the other hand, in Fig. 2-2, we cannot see the magnified group 3 of the USAF 1951 target as much as with the GRIN lens when the imaging lens with a 0.23 pitch is arrayed in the FOG because the working distance of an imaging lens is designed to be 0 mm. However, we could acquire optical images of the USAF 1951 target with a higher contrast and sharpness as shown in Fig. 3. Figure 3 shows measured MTF curves when combining only one type of GRIN lens and imaging lens. Therefore, we concluded that the imaging lens was suitable for our FOG system. Incidentally, in Fig. 2-3, the optical image through the FOG was obtained with lower spatial resolution as compared to when only one type of imaging lens was used. When an image is transmitted, a greater number of optical interfaces create more crosstalk and leaky rays, reducing the contrast and resolution.

The MTF can be used to evaluate the spatial resolution and contrast of a fiber-optic imaging system. The MTF curve of the imaging system was calculated from the Fourier transform of the line spread function (LSF), which is the derivative of the edge response function (ERF). Through Fig. 4, which shows the comparison of the MTF curves when combining only one type of imaging lens and the additional optical elements combined in the

FOGE, we can discern the rate of decline of the spatial resolution. The reason for these trends is that the MTF is a parameter that determines the overall performance of the entire imaging system and there is interference of the light and leaky rays between the optical interfaces when the scintillator disc and UV filter film are combined.

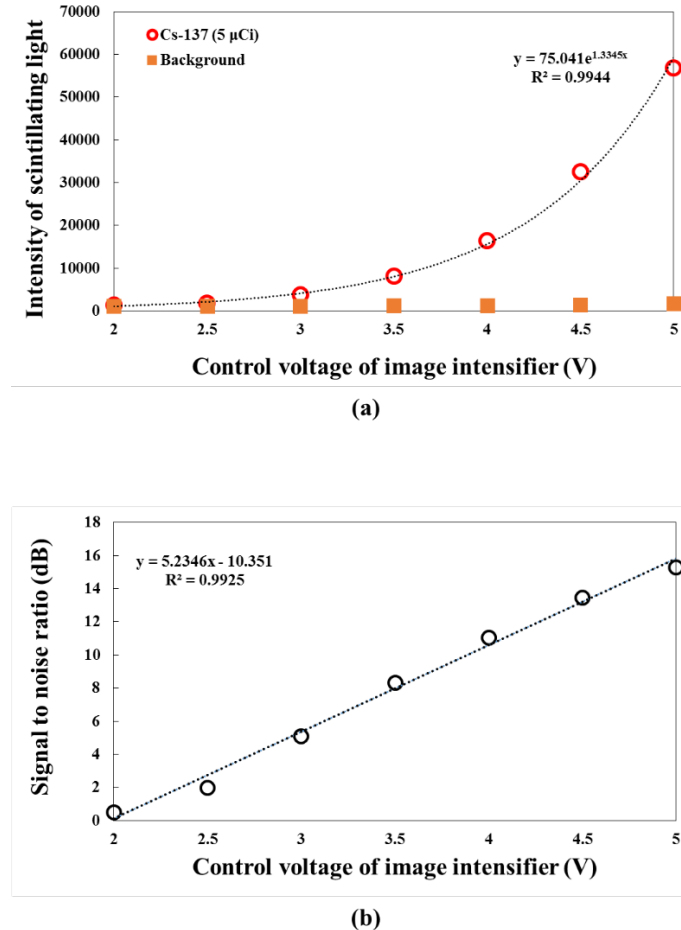


Fig. 5. (a) The intensities of the scintillating light and (b) SNR as a function of the control voltage of the image intensifier.

Figure 5(a) shows the intensities of the scintillating light emitted from the LYSO:Ce in FOGE as functions of the control voltages applied to the image intensifier. As shown in Fig. 5(b), the spectral gain and signal-to-noise ratio (SNR) of the image intensifier increase as the control voltage increases. However, the control voltage depends on the energy and radioactivity of the radioisotope to be measured. Therefore, we can obtain the optimal gamma images with a proper control voltage for the image intensifier, which can enhance the image quality of the FOGE.

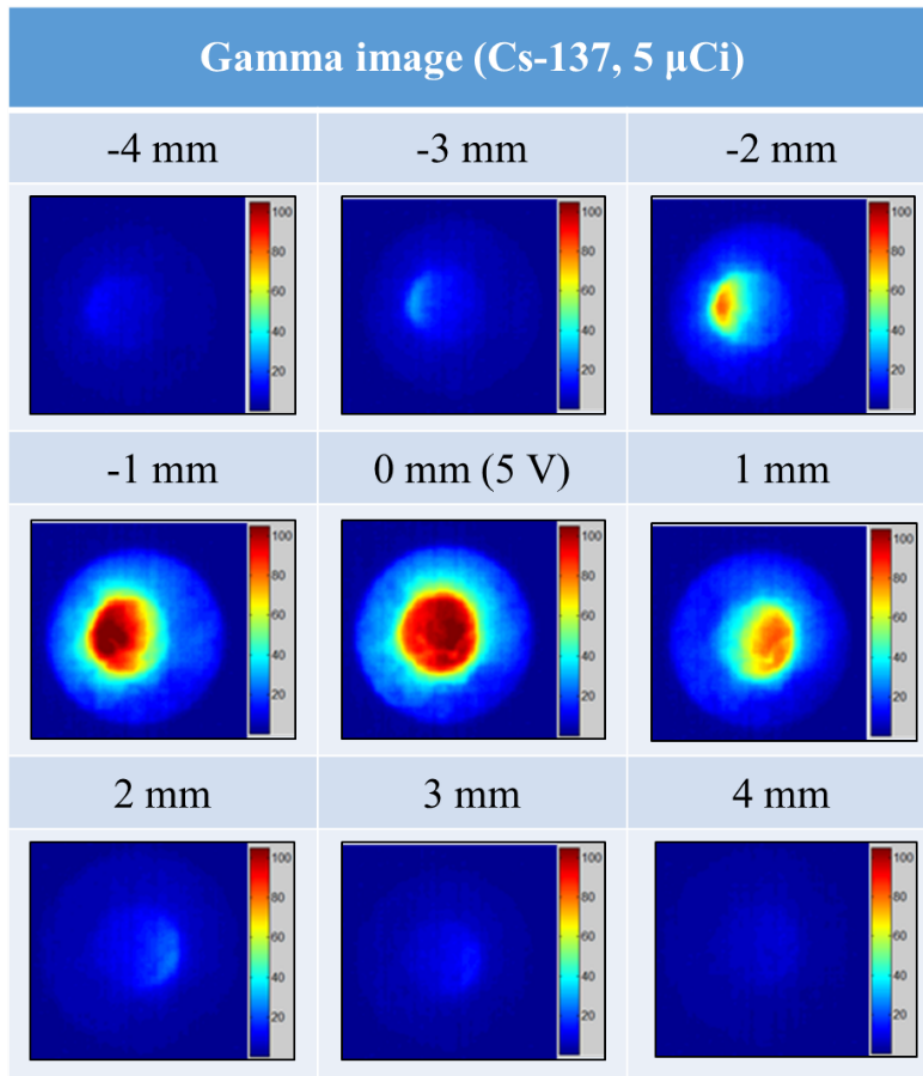
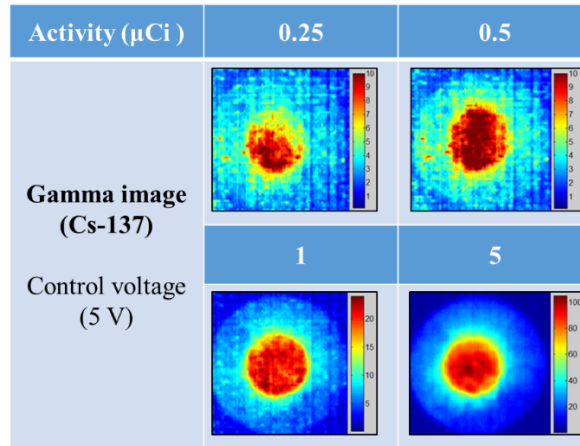
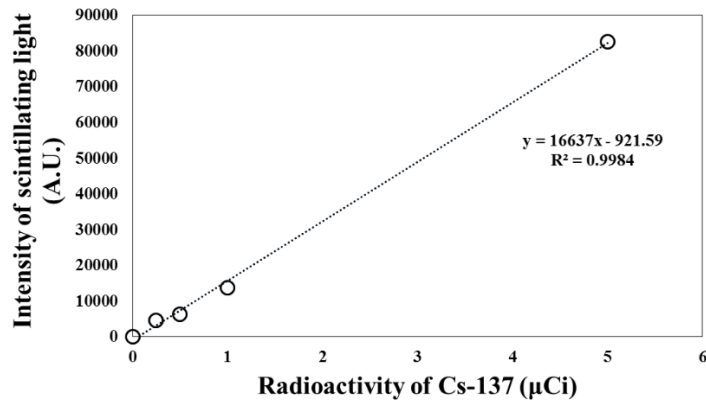


Fig. 6. Gamma images according to the location of the radioisotope.

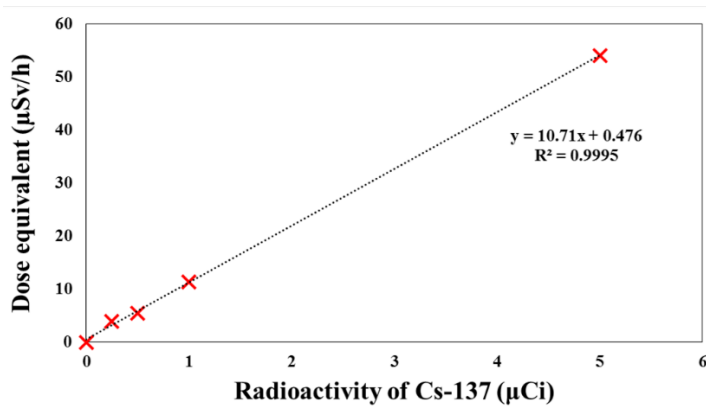
Figure 6 shows the gamma images and gamma distributions according to the location of Cs-137 with 5 μ Ci of radioactivity when using the FOG. We can see that the position of the gamma distribution is slightly shifted when the source is moved 1 mm from the probe, either to the left or to the right.



(a)



(b)



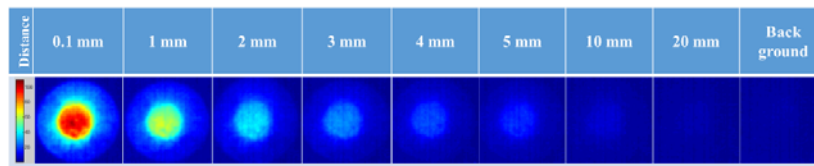
(c)

Fig. 7. (a) Gamma images, (b) intensity of the scintillating light, and (c) dose equivalent according to the radioactivity of the radioisotope.

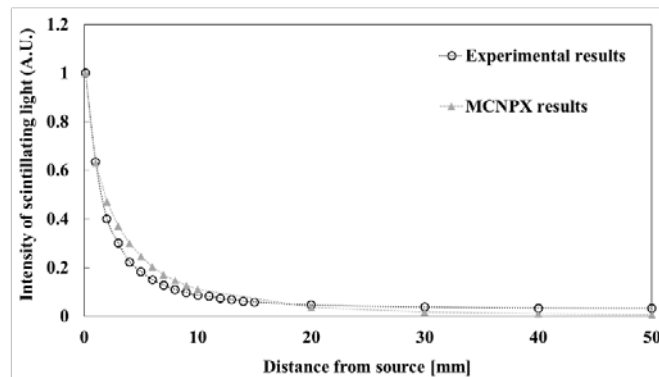
Figure 7 shows the variation of the gamma images, intensity of the scintillating light, and dose equivalent according to the radioactivity of the radioisotope. The radioisotope Cs-137 with radioactivities of 0.25, 0.5, 1, and 5 μCi was used. The gamma-ray distribution of Cs-137 with a low level radioactivity of 0.25 μCi was measured, and it was confirmed that the FOGE has high sensitivity in gamma imaging. To obtain the plots in Fig. 7(b), we assigned a region of interest (ROI) in the gamma images after superimposing real-time images and converting them into an RGB scale to analyze the intensity of the scintillating light. The circular ROI is assigned to the field of view of the FOGE with pixels of 62.5 μm in size. Figure 7(c) shows the dose equivalent of Cs-137 according to the radioactivity measured by using a commercial survey meter (X5C plus, GRAETZ Strahlungsmeßtechnik GmbH). Based on Figs. 7(b), (c), the light intensity and dose equivalent according to the radioisotope have a linear relationship. Thus, the novel FOGE in this study has a linear response that can facilitate the dose measuring of gamma-rays from the gamma imaging. Accordingly, we derived the equation, as shown below, that can be used to convert the data on the light intensity of the scintillation signal to dose equivalents by using the gamma images acquired through the FOGE.

$$D\left(\frac{\mu\text{Sv}}{\text{h}}\right) = \frac{10.71I - 9870.23}{16637} + 0.476 \quad (1)$$

where I is the intensity of the scintillating light emitted from the LYSO:Ce disc in the FOGE, and D is the dose equivalent. According to the above equation, even if a very short half-life isotope such as Tc-99m (6 h) is used in treatment or diagnosis during nuclear medicine applications, the dose equivalent for the patient can be calculated by using the FOGE in real time.



(a)



(b)

Fig. 8. (a) Gamma images and (b) intensity of the scintillating light and MCNPX results as a function of the distance between the radioisotope and the FOGE.

Figure 8(a) shows gamma images taken when the distance between the Cs-137 radioisotope with a 5 μCi of radioactivity and the FOGE is changed when the control voltage of the image intensifier is set to 5V. As the distance between the tip of the FOGE and the

surface of Cs-137 increases, the intensity of the scintillation image is reduced and the blurring of the scintillation image is increased due to the gamma-rays emitted from the radioisotope, which traveled in all directions and attenuated in air. When the distance is greater than 20 mm, it is almost the same as the background gamma image. It can be seen that the gamma-ray is barely incident on the FOG.

Figure 8(b) shows the variation in intensity of the scintillation signal and Monte Carlo N-particle transport code (MCNPX) results according to the distance between the Cs-137 with a radioactivity of 5 μCi and the tip of the FOG. According to the results, the intensity of the scintillation signal decreases in inverse proportion to the square of the distance. It has an intensity of about 60% when the distance is 1 mm, but at a distance of 20 mm from the source, the measured intensity of scintillating light is almost zero. However, if the energy and radioactivity of the radiation source to be measured are large, and the diameter of the scintillator used in the FOG becomes large, the measurable distance will increase [29].

4. Conclusion

In this study, we proposed a new type of surgical probe for MIRS that could yield various advantages such as reduced costs and operative times, limited dissections with fewer complications and smaller incisions, and comparable operative success rates. We fabricated a novel FOG by using UV filter film, a scintillator disc, an imaging lens, a fiber-optic image guide, a fiber-optic taper, an image intensifier, and a CMOS (complementary metal-oxide semiconductor) camera module, and this setup can measure not only the shape and size of the radioisotope but also the gamma-ray distribution simultaneously. Our proposed FOG can be used to find exact location of the tumor or tumor remnant using optical and gamma images by changing final optical device such a CMOS camera and an image intensifier, respectively. Further, we obtained optical images of a USAF 1951 target and gamma images of Cs-137 radioisotopes. To evaluate the spatial resolutions of the FOG system, MTFs were calculated based on the LSFs and ERFs of the optical images. The numeric value of the light intensity and dose equivalent were also calculated based on the gamma images, which reveal the distribution and intensity of the radioisotope. Finally, we were able to obtain the optical and gamma images with a very simple method by using the novel FOG system. The proposed novel FOG has a diameter of 2 mm, which is smaller than the minimum diameter of 5 mm of currently used gamma probes, and the new probe is flexible. We expect that it will be easy to make available and will allow for easy and accurate intraoperative identifications of radiopharmaceuticals distributed over whole abnormal lesions when a small surgical access area is made in minimally invasive approaches such as MIRS. In addition, since the novel FOG can be used to measure optical images and scintillation images simultaneously during MIRS, it should be easy to operate by surgeons who have experience in radioguided surgery with the exploration method. In summary, the new endoscope has the potential to make MIRS surgery safer and more readily commercialized.

Further studies will be carried out to obtain a more enhanced field of vision and information on other gamma images by using a wide-angle lens and compact collimators.

Funding

Basic Science Research Program (No. 2017R1A2B2009480); National Nuclear R&D Program (No. 2016M2B2B1945255) through the National Research Foundation of Korea (NRF) funded by the Ministry of Science, ICT, and Future Planning.